siRNA Delivery

DOI: 10.1002/ange.201201390

Tumor-Homing Poly-siRNA/Glycol Chitosan Self-Cross-Linked Nanoparticles for Systemic siRNA Delivery in Cancer Treatment**

So Jin Lee, Myung Sook Huh, Seung Young Lee, Solki Min, Seulki Lee, Heebeom Koo, Jun-Uk Chu, Kyung Eun Lee, Hyesung Jeon, Yongseok Choi, Kuiwon Choi, Youngro Byun, Seo Young Jeong, Kinam Park, Kwangmeyung Kim, and Ick Chan Kwon**

A key challenge for the therapeutic use of small interfering RNA (siRNA) in clinical fields is delivery of the siRNA to the cytosol of target cells within targeted tissues. Therefore, various siRNA delivery systems, such as liposomes, polymers, and inorganic particles, have been developed to improve the therapeutic efficacy of siRNA.[1] In particular, nanoparticle-based delivery systems with size ranges of 100–500 nm are known to efficiently accumulate at tumor sites through fenestrate vasculature, this phenomenon is called the enhanced permeation and retention (EPR) effect.[2] However, nanoparticles based on charge–charge interactions between cationic molecules and anionic siRNAs have proven unsatisfactory, mainly because of their insufficient in vivo stability and low tumor-targeting efficacy in cancer treatment.[3]

The most important problem in current siRNA delivery systems is their inability to form condensed nanoparticles with cationic lipids or polymers. This situation may be because of the low charge density and molecular weight of short double-stranded siRNAs compared to plasmid DNA, which can form a very stable and condensed nanoparticle structure with cationic molecules. It has been reported that siRNAs that are loosely bound to nanoparticles can be easily attacked by several enzymes in the blood and rapidly degraded before arrival at the targeted tumor tissues. Furthermore, with strong cationic polymers, such as polyethylenimine (PEI), undesirable cytotoxicity and non-specific targeting in normal liver or spleen greatly limits their therapeutic use.

To achieve efficient delivery, alternative strategies to increase the molecular weight of siRNAs have been suggested. Oligomerized or polymerized siRNAs with higher molecular weight and anionic charges could form stable and condensed nanoparticle structures with cationic polymers, resulting in enhanced stability and efficient delivery. For example, Behr and co-workers showed that siRNAs with short complementary overhangs could generate sticky siRNAs (ssiRNA) by annealing to each other.[4] On the other hand, Park and co-workers and our group reported that chemically cross-linked siRNAs, such as multimeric siRNAs or polymerized siRNAs (poly-siRNA), could be successfully prepared by introducing a disulfide linkage at the 5′ end of each siRNA strand.[5] Importantly, these higher molecular weight siRNAs, when complexed with polymeric carriers, greatly increase the stability of the nanoparticle structure under physiological conditions. However, systemic delivery of nanoparticles with multimeric or polymerized siRNAs in cancer treatment has not been well studied.

Herein, we designed and synthesized a novel self-cross-linking nanoparticle to deliver polymerized siRNAs for cancer treatment. Poly-siRNA, with an average of 12 siRNAs linked, can easily form a stable nanoparticle structure with thiolated glycol chitosan (TGC) polymers through charge–charge interaction and chemical cross-linking. To investigate the potential use of the resulting self-cross-linked poly-siRNA glycol chitosan nanoparticles (psi-TGC) as a new siRNA delivery system, we evaluated its enhanced stability and gene silencing efficacy in vitro. Furthermore, in vivo tumor targeting and gene silencing efficacy of psi-TGC were evaluated after intravenous injection into tumor-bearing mice.

Poly-siRNA, with reducible disulfide linkages, was prepared through self-polymerization of thiol groups at the 5′ end of each sense strand and antisense strand of the siRNAs (Scheme 1 a).[5b] Thiol-modified sense and antisense strands of siRNA were annealed and self-polymerized under mild oxidation and basic conditions in HEPES buffer (pH 8.0). To stabilize and condense poly-siRNA carriers, the primary amine groups of glycol chitosan (GC) polymers were partially modified into thiols with sulfosuccinimidyl-6-(3′-[2-pyridyldi-

[*] S. J. Lee,[+] Dr. M. S. Huh,[+] S. Y. Lee, S. Min, Dr. S. Lee, Dr. H. Koo, Dr. J.-U. Chu, Dr. K. E. Lee, Dr. H. Jeon, Dr. K. Choi, Dr. K. Kim, Dr. I. C. Kwon
Center for Theragnosis, Biomedical Research Institute, Korea Institute of Science and Technology
39-1 Hawolgok-dong, Seongbuk-gu, Seoul 136-791 (Korea)
E-mail: kim@kist.re.kr
ikwon@kist.re.kr
S. Y. Lee, Dr. Y. Choi
School of Life Science and Biotechnology, Korea University (Korea)
Dr. Y. Byun
Department of Molecular Medicine and Biopharmaceutical Sciences, Seoul National University (Korea)
Dr. S. Y. Jeong
Department of Life and Nanopharmaceutical Science, Kyung Hee University (Korea)
Dr. K. Park
Departments of Biomedical Engineering and Pharmaceutics, Purdue University (USA)
[+] These authors contributed equally to this work.

[**] This study was funded by the Global Research Laboratory (GRL) Project, the Fusion Technology Project (2010-50201), and the Intramural Research Program (Global RNAi Initiative) of KIST.
Supporting information for this article (experimental details) is available on the WWW under http://dx.doi.org/10.1002/anie.201201390.

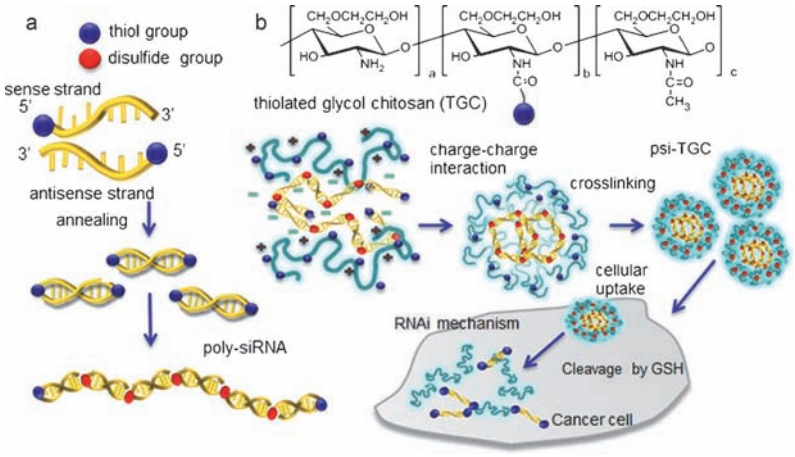

Scheme 1. Schematic diagram of a) poly-siRNA and b) poly-siRNA/glycol chitosan nanoparticles for siRNA delivery in cancer treatment.

thio]-propionamido)hexanoate (sulfo-LC-SPDP) and reduced with dithiothreitol (DTT; Supporting Information, Figure S1). After adding anionic poly-siRNA to the solution containing cationic thiolated GC polymers, weak charge–charge interactions occurred between them, resulting in loosely bound large structures (Scheme 1 b). The binding (charge interaction) of the poly-siRNAs to the thiolated GC polymers decreases the distances of the thiol groups between them, allowing the thiolated GC polymers to undergo intramolecular cross-linking, which formed more condensed nanostructures.

To make self-cross-linked poly-siRNA/glycol chitosan nanoparticles (psi-TGC), poly-siRNA in HEPES buffer was slowly added to the thiolated GC polymers for 1 h at 37 °C. The GC/siRNA weight ratio was either 5% or 10%. . The poly-siRNA showed a ladder-like migration pattern by 8% native polyacrylamide gel electrophoresis (PAGE), indicating their lengths are from 50 basepairs (bp) to above 300 bp (Figure 1 a). The intensity of each gel band for poly-siRNA was quantitatively analyzed and showed that about 70% of the poly-siRNA was above 300 bp in length. On average, poly-siRNA, has 12 times more anionic charge per molecule than mono-siRNA. In a gel retardation assay, psi-TGC produced stable complexes, at a weight ratio of 1:5 (poly-siRNA/TGC) while the stability was lower in the case of poly-siRNA/non-thiolated GC complex (psi-GC; Figure 1 b, Figure S2 a). Importantly, both poly-siRNA and psi-TGC was successfully degraded and separated into monomeric double-stranded siRNAs after adding 10 mM of DTT for 30 minutes. This result demonstrates that psi-TGC could release free siRNAs under reductive conditions, such as those found in the cell cytosol, even after polymerization and complexation with thiolated GC. Under optimal conditions, 7% of amine residues on GC polymers were modified with thiol groups for making psi-TGC (Figure S2 b).

TEM and cryo TEM images demonstrated that psi-TGC had a more condensed structure than psi-GC and we believe this is due to the chemical cross-linking of thiolated GC polymers in the nanoparticles (Figure 1 c). These images revealed similar spherical morphology of both complexes but different sizes, where psi-TGC was smaller than non-thiolated psi-GC controls. The average hydrodynamic diameters of psi-TGC was about 300 nm as measured by dynamic light scattering (DLS, Figure 1 d), and their surface was slightly positive (ξ potential $= 3.55 \pm 0.58$ mV; Table S1). However, psi-GC complexes have a larger size and broad distribution compared to psi-TGC, showing that chemical cross-linking of thiolated GC polymers plays a pivotal role in the fabrication of condensed nanoparticles. The stability of psi-TGC against physiological anionic proteins or carbohydrates was evaluated through a heparin decomplexation assay. After incubation with heparin, psi-TGC showed better stability than psi-PEI, which forms a complex only through charge–charge interactions (Figure 1 e). In 10% FBS containing HEPES buffer, non-polymerized mono-siRNA was degraded within 1 h, whereas the degradation of poly-siRNA was not complete after 6 h (Figure 1 f).

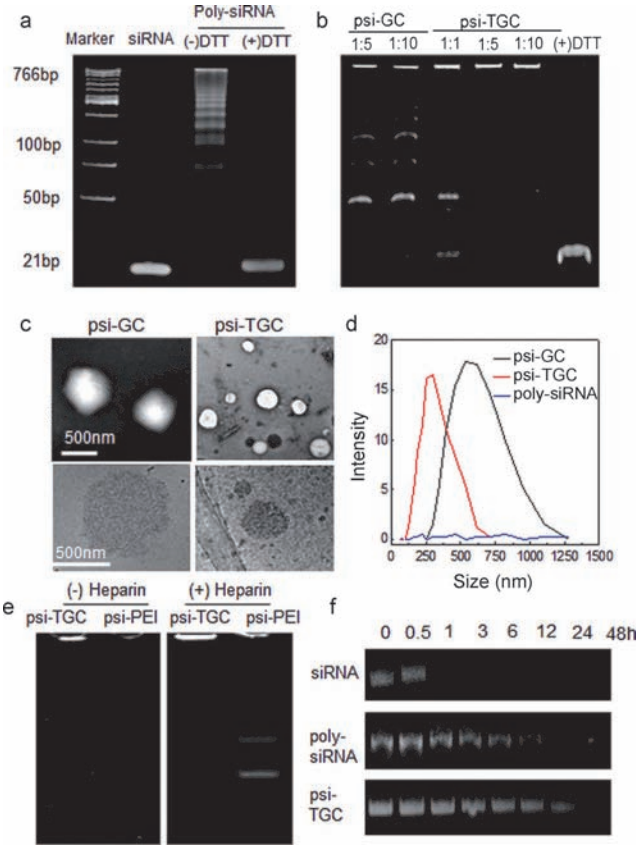

Figure 1. Development of psi-TGC and physicochemical characterization. a) Confirmation of poly-siRNA formation by gel electrophoresis of mono-siRNA, poly-siRNA, and reduction of poly-siRNA by adding DTT. b) Gel retardation assay of complexes of GC or thiolated GC with poly-siRNA at different weight ratios (1:1, 1:5, and 1:10 GC/siRNA). c) TEM (top) and cryo TEM (bottom) images and d) dynamic light scattering (DLS) of psi-TGC. e) Stability of psi-TGC and psi-PEI before and after treatment with heparin and DTT. f) Serum stability of mono-siRNA, poly-siRNA, and psi-TGC in 10% FBS containing HEPES buffer.

However, psi-TGC was still present even after 24 h incubation showing its superior stability against serum nucleases. These data show that psi-TGC has enhanced stability owing to the successful encapsulation of poly-siRNA into TGC. Therefore, we hypothesize that psi-TGC would be stable in the blood and then, after cellular uptake, degraded into monomeric siRNAs in the cytosol for gene silencing.

The cellular uptake of psi-TGC was monitored in B16F10 cells with confocal microscopy, wherein thiolated GC was labeled with FITC (green) and poly-siRNA was labeled with near infrared fluorescence (NIRF) dye (red), FPR675. As shown in Figure 2a, distinct green and red spots of GC and poly-siRNAs indicate the rapid internalization and localization of psi-TGC in cytosol within 1 h. Compared to the faint NIRF signals of free poly-siRNA, cellular uptake is greatly enhanced by the stable condensed nanostructure of psi-TGC. Additionally, our previous study demonstrated that GC nanoparticles can be internalized into cell cytoplasm by way of various endocytotic or macropinocytosis pathways, [6] which further explains this fast cellular uptake of psi-TGC. To investigate in vitro gene silencing efficacy of psi-TGC, we used psi-TGC targeting red fluorescent protein (RFP) in RFP-expressing B16F10 cells. In microscopic images, the red fluorescence signals of RFP/B16F10 cells treated with psi(RFP)-TGC (100 nM of siRNA) were highly reduced compared to psi(RFP)/Lipofectamine 2000 (LF), a commercial transfection reagent (Figure 2b). No significant fluorescence changes with scrambled sequence psi-TGC (psi(sc)-TGC) shows that the RFP suppression by psi(RFP)-TGC is sequence specific. In quantitative analysis of RFP mRNA by real-time RT-PCR, 100 nM of psi(RFP)-TGC treatment efficiently suppressed RFP expression to 74%, comparable to that of psi(RFP)/LF treatment (73%; Figure 2c). Also, to test the therapeutic potential of psi-TGC in cellular conditions, we prepared psi-TGC targeting the vascular endothelial growth factor (VEGF) sequence.[5a] Using the same synthetic procedure, stable complexes of psi(VEGF)-TGC were obtained and they showed an excellent VEGF gene silencing efficacy of about 95% in PC-3 cells (Figure S3). These results indicate that psi-TGC can effectively silence a target gene with fast cellular uptake in a sequence-specific manner. The variance in the gene-silencing efficiencies of psi(RFP)-TGC and psi(VEGF)-TGC may be due to the different gene expression levels of RFP and VEGF (Figure S3).

To evaluate the enhanced stability and tumor-targeting ability of psi-TGC in vivo, time-dependent biodistribution of the psi-TGC was monitored by fluorescent imaging after intravenous injection into SCC-7 tumor-bearing mice (Figure 3a). When the tumor size reached to 6–8 mm, psi-TGC containing 50 μg of FPR675-labeled poly-siRNA was injected into the mice through the tail vein. The mice showed a strong NIRF signal throughout the whole body within 1 h post-injection, indicating that psi-TGC stably circulated in the bloodstream. Subcutaneous tumors could be delineated from the surrounding tissue 3 h post-injection. The maximum NIRF signal in tumor tissue was shown at 1 day post-injection and it persisted for up to 3 days compared to other tissues. Quantitative analysis of NIRF signals showed that psi-TGC accumulated in tumor tissue fourfold more than free poly-siRNA (Figure 3b). As controls, free poly-siRNA and psi-PEIs injected into mice did not show any remarkable increase of NIRF signals at the tumor site during 3 days post-injection. Although PEI has been shown to condense into compact nanoparticles and its transfection efficiency is high, most psi-PEIs were found in the liver, showing negligible accumulation

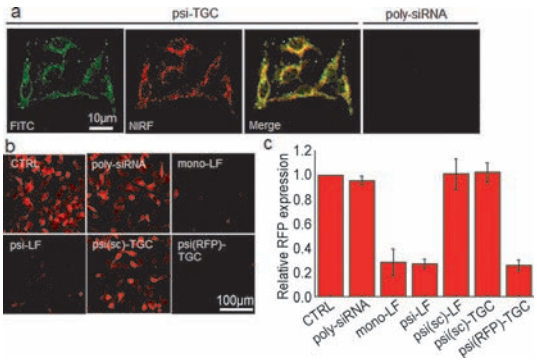

Figure 2. In vitro cellular uptake and gene silencing efficacy of psi-TGC. a) Confocal microscopic images of B16F10 cells treated with psi-TGC with FITC-labeled thiolated GC (green) and FPR675 labeled poly-siRNA (red). RFP/B16F10 cells were treated with psi(RFP)-TGC and psi(sc)-TGC (siRNA concentration = 100 nM) for 48 h. Controls with no siRNA added (CTRL), poly-siRNA alone, mono-siRNA with LF and poly-siRNA with LF were also performed. b) Fluorescence microscopic images and c) real-time RT-PCR data obtained at 2 days post-incubation with poly-siRNA formulations.

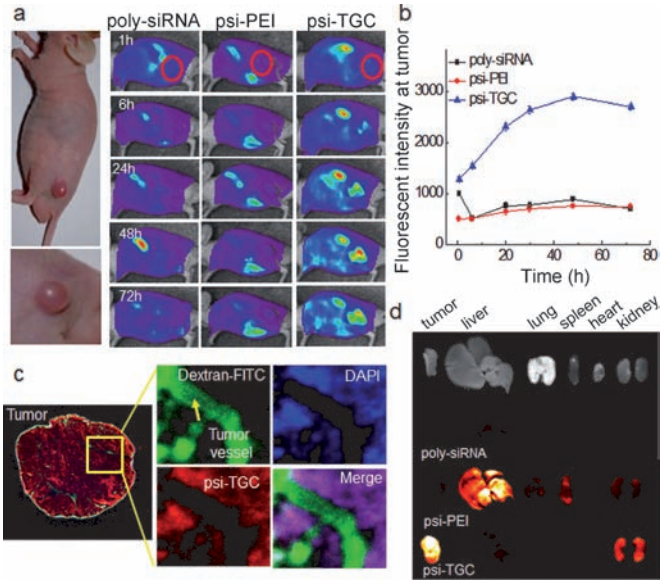

Figure 3. In vivo real-time NIRF imaging of psi-TGC in tumor-bearing mice. a) Whole-body imaging of the SCC-7 tumor bearing mice after intravenous injection of FPR675-psi-TGC was performed for up to 3 days. Also, control mice injected with poly-siRNA or psi-PEI were imaged. Red circle = site of tumor. b) Fluorescence intensity of FPR675-poly-siRNA at the tumor site ($n = 3$ mice per group). c) Intravital image of tumor tissue penetrated with FPR675-psi-TGC. Tumor tissue and vasculature were visualized after injection of FITC-dextran by tail vein, and then tumor tissues were excised and stained with DAPI solution. d) Ex vivo NIRF images of dissected organs 3 days post-injection.

in tumor tissue. In addition, the optimal degree of thiolation of psi-TGC was found to be 7%, in comparison to the in vivo biodistribution of 2% psi-TGC in NIRF images (Figure S4).

High-resolution images of blood vessels in tumor tissue showed that psi-TGC were mainly co-localized with SCC7 tumor cells (blue color with DAPI stain) 1 hour post-injection, not with tumor blood vessels (green color with FITC labeled dextran), indicating their cellular penetration through leakage from tumor blood vessels and quick uptake into tumor cells(Figure 3d). Three days post-injection, each organ (liver, lung, spleen, kidney, heart, and tumor) was excised to compare the organ distribution of psi-TGC in tumor-bearing mice. As expected, psi-TGC treated mice showed the strongest NIRF signals in tumor tissue among all excised organs, and this accumulation in tumor tissue was not observed in the case of free poly-siRNA and psi-PEIs (Figure 3d). Moreover, the total fluorescent photon counts from tumor tissue were about 2.1- to 9.8-fold higher than those from other organs in case of psi-TGC (Figure S7). The significant retention of psi-TGC in the kidneys originates from its longer blood circulation time compared to free siRNAs. However, the retention of psi-TGC in the kidneys is not a serious problem because they are generally excreted from the body several days post-injection.

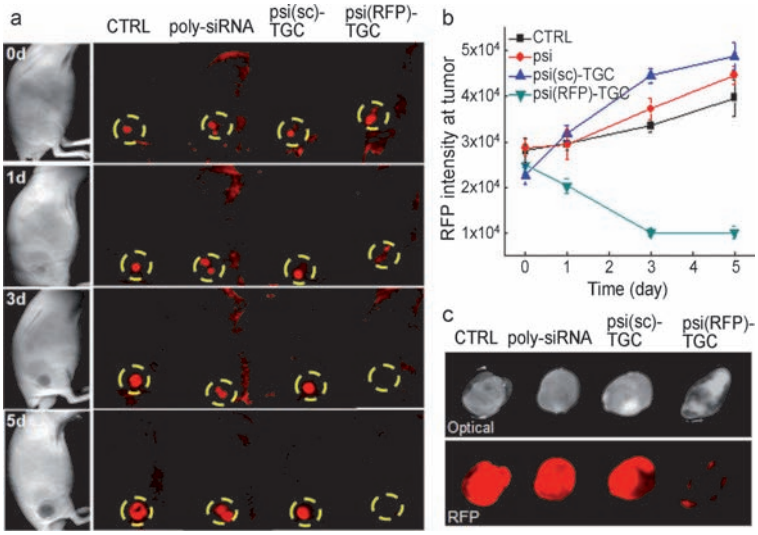

Figure 4. In vivo gene silencing effects of psi(RFP)-TGC in RFP/B16F10 tumor-bearing mice. a) Fluorescent imaging of RFP gene silencing from psi-TGC treated mice. Each mouse was systemically injected with 50 μg of siRNA every 2 days (days 0, 2, and 4). Yellow circle = tumor site. b) Measured RFP intensity at tumor tissue ($n = 3$). Data represents average ± s.d. from 3 mice. c) Ex vivo imaging of the excised RFP/B16F10 tumors 5 days post-injection.

To evaluate the in vivo gene silencing efficacy of psi-TGC, real-time non-invasive fluorescence images were obtained in RFP-B16F10 tumor-bearing mice treated with psi(RFP)-TGC. When the RFP-expressing tumors grew to 3–5 mm in diameter, psi(RFP)-TGC (50 μg of siRNA/mouse) was intravenously injected into the mice every other day and gene silencing was monitored by measuring RFP signal intensity in tumors. Figure 4a,b shows that the RFP signal clearly diminished to about 17% after psi(RFP)-TGC administration, compared to control mice. Free poly-siRNA and psi(sc)-TGC injected mice retained their intense RFP fluorescence at the tumor site, showing negligible gene silencing. In excised tumors, RFP silencing of psi(RFP)-TGC was significantly higher, compared to the controls of free poly-siRNA and psi(sc)-TGC (Figure 4c). This reduction of RFP signal was also confirmed by histological examination (Figure S8).

Finally, we evaluated the therapeutic efficacy of psi-(VEGF)-TGC in tumor-bearing mice, which is predicted to suppress tumor growth and angiogenesis. Psi(VEGF)-TGC were intravenously injected into the PC-3 tumor xenograft mice every 3 days. As shown in Figure 5a,b, psi(VEGF)-TGC treated mice had significantly reduced tumor volumes (by 80%) as compared to the control group ($p < 0.05$). Free poly-siRNA or psi(sc)-TGC treated groups had tumor volumes similar to control mice, indicating that the tumor suppression of psi-TGC was sequence-specific. Live imaging of blood vessels in tumor tissue showed active formation of large blood vessels with free poly-siRNA or psi(sc)-TGC treatment (Figure 5c). However, microvessel formation in tumor tissue of psi-(VEGF)-TGC treated mice was significantly reduced. This indicates that the tumor growth inhibition originated from VEGF gene silencing and inhibited angiogenesis. Reduced microvessels in the psi(VEGF)-TGC treated group were observed in both CD31 and Von Willebrand factor (vWF) stained tissue images (Figure S9a). Microvessel density was counted based on vWF positive endothelia, and a significant difference ($p < 0.05$) was detected between the psi(VEGF)-TGC treated group and the control group (35.1 ± 4.2 versus

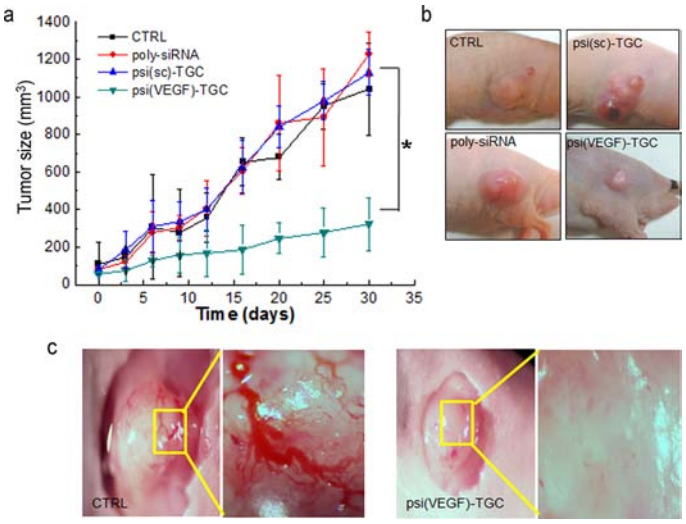

Figure 5. In vivo tumor therapy with systemic administration of psi(VEGF)-TGC in PC-3 tumor-bearing mice. a) Tumor growth was measured for 24 days after treatment at 3 day intervals with no siRNA (CTRL), free poly-siRNA, psi(sc)-TGC, or psi(VEGF)-TGC. b) Images of tumors from the groups described in (a) at 10 days. c) Blood vessel development was monitored using an OV-100 imaging system in control and psi(VEGF)-TGC treated tumors.

62.6 ± 11.3 microvessels mm^{-2}, respectively; Figure S9b). We verified that this remarkable reduction of microvessel formation was correlated with the suppression of VEGF gene expression by RT-PCR. The amount of VEGF mRNA in the psi-TGC treated group was decreased to about 35.9% of that in control group, while free poly-siRNAs or psi(sc)-TGC treated groups showed no significant changes (Figure S9c). In addition, we tested the immune response of mice treated with psi-TGC by measuring the expression of IL-6, a pro-inflammatory cytokine. Human prostate cancer PC-3 cells were treated with free poly-siRNA, psi-TGC, psi-LF, thiolated GC, or poly(I:C), an inflammatory stimulant (Figure S10). Significant amounts of cytokine secretion were detected only in poly(I:C)-treated cells, while there was no noticeable change in all other groups compared to nontreated control cells. This result shows that the poly-siRNA, thiolated GC, and combined psi-TGC do not trigger immune stimulation and could be safe for clinical applications.

In summary, we have shown that thiolated glycol chitosan can form stable nanoparticles with poly-siRNA through charge–charge interactions and self-cross-linking, simultaneously. This structure provided sufficient stability from nucleases while still allowing for mono-siRNA release in the cytosol upon systemic delivery of poly-siRNA. The stable nanostructure of psi-TGC especially enabled tumor-targeted delivery and quick uptake into tumor cells for efficient gene silencing. With this psi-TGC, we showed in vivo VEGF gene silencing and reduced angiogenesis in tumors by treating with small amounts of siRNA. Considering the current interest in siRNAs and the number of hurdles in their biomedical application, psi-TGC has great potential as an siRNA delivery system for tumor therapy.

Received: February 20, 2012
Revised: April 10, 2012
Published online: June 13, 2012

Keywords: antitumor agents · glycol chitosan · nanoparticles · poly-siRNA · siRNA delivery

[1] K. A. Whitehead, R. Langer, D. G. Anderson, *Nat. Rev. Drug Discovery* **2009**, *8*, 129 – 138.
[2] V. Torchilin, *Adv. Drug Delivery Rev.* **2011**, *63*, 131 – 135.
[3] Y.-K. Oh, T. G. Park, *Adv. Drug Delivery Rev.* **2009**, *61*, 850 – 862.
[4] A.-L. Bolcato-Bellemin, M.-E. Bonnet, G. Creusat, P. Erbacher, J.-P. Behr, *Proc. Natl. Acad. Sci. USA* **2007**, *104*, 16050 – 16055.
[5] a) H. Mok, S. H. Lee, J. W. Park, T. G. Park, *Nat. Mater.* **2010**, *9*, 272 – 278; b) S.-Y. Lee, M. S. Huh, S. Lee, S. J. Lee, H. Chung, J. H. Park, Y.-K. Oh, K. Choi, K. Kim, I. C. Kwon, *J. Controlled Release* **2010**, *141*, 339 – 346.
[6] H. Y. Nam, S. M. Kwon, H. Chung, S.-Y. Lee, S.-H. Kwon, H. Jeon, Y. Kim, J. H. Park, J. Kim, S. Her, Y.-K. Oh, I. C. Kwon, K. Kim, S. Y. Jeong, *J. Controlled Release* **2009**, *135*, 259 – 267.